Characterization of hydrogen bond acceptor molecules at the water surface using near-edge

x-ray absorption fine-structure spectroscopy and density functional theory

LETTER TO THE EDITOR

Characterization of hydrogen bond acceptor molecules at the water surface using near-edge x-ray absorption fine-structure spectroscopy and density functional theory

Kevin R Wilson[1]**, Matteo Cavalleri**[3]**, Bruce S Rude**[2]**,**
Richard D Schaller[1]**, A Nilsson**[4,5]**, L G M Pettersson**[3]** N Goldman**[1]**, Tony**
Catalano[2]**, J D Bozek**[2]** and R J Saykally**[1,6]

[1] Department of Chemistry, University of California, Berkeley, CA 94720, USA
[2] Advanced Light Source, Lawrence Berkeley National Laboratory, Berkeley, CA 94720, USA
[3] FYSIKUM, Stockholm University, Box 6730, S-113 85 Stockholm, Sweden
[4] Department of Physics, Uppsala University, Box 530, S-751 21, Uppsala, Sweden
[5] Stanford Synchrotron Radiation Laboratory, 2575 Sand Hill Road, Menlo Park, CA 94025, USA

E-mail: saykally@uclink4.berkeley.edu

Abstract
We present a combined experimental/computational study of the near-edge
x-ray absorption fine structure of the liquid water surface which indicates that
molecules with acceptor-only hydrogen bonding configurations constitute an
important and previously unidentified component of the liquid/vapour interface.

A detailed microscopic picture of the liquid water surface underlies many important
phenomena, ranging from the terrestrial CO_2 and H_2O cycles to surface wetting and ice
formation. Surface hydrogen bond configurations, which determine important interfacial
properties, e.g. surface tension and interfacial mobility, remain incompletely characterized.
Molecular dynamics (MD) simulations of water molecules residing in the $\sim$5 Å [1]
liquid–vapour interface have revealed an overall relaxation of bulk properties (e.g. dipole
moment, geometry, diffusion constant, density) toward gas-phase values, precipitated by the
disintegration of the three-dimensional liquid hydrogen bond network [2–5]. Sum frequency
generation (SFG) studies have provided the first important experimental insights into the
molecular details of the liquid water surface. Shen and co-workers [6] report a vibrational
band slightly red-shifted from the gas-phase symmetric stretch of water vapour consistent with
a free O–H oscillator. They further concluded that >20% of the surface molecules are oriented
with one free O–H bond extending out of the surface by about 38°.

[6] Author to whom any correspondence should be addressed.

Near-edge x-ray absorption fine structure (NEXAFS) and extended x-ray absorption fine structure (EXAFS) yield information on the instantaneous local electronic structure as well as spatial correlations among neighbouring molecules. Our recent measurements [7] of the EXAFS spectrum of the liquid water surface indicate an overall relaxation of the average O–O distance to 3.00 ± 0.05 Å from a bulk value of 2.85 ± 0.05 Å, consistent with interfacial molecules interacting more weakly and over larger distances. Here we report the corresponding analysis of the oxygen K-edge NEXAFS spectrum which provides new insight into the local hydrogen bond configurations of water molecules residing at the liquid water surface.

It is well known in the field of core-level spectroscopy that electrons or ions emitted from a material by photon or electron excitation probe different regions of a sample, determined by the relative escape depths of these particles [8]. Total-electron-yield measurements are dominated by a secondary-electron cascade which escapes into vacuum from an average depth of 25 Å, thereby probing many monolayers. Conversely, ions are ejected into vacuum by a Coulomb desorption mechanism which is primarily sensitive to the outermost surface layer (1–5 Å) [9]. This phenomenon, generally known as desorption induced by electronic transition (DIET) for both photon and electron excitation, has been extensively characterized for monolayer adsorbates as well as condensed-phase systems [10].

Oxygen K-edge (530 eV) spectra of liquid microjets were measured on beamline 8.0 at the Advanced Light Source, Lawrence Berkeley National Laboratory. The small spot size (100×100 μm) and high flux (10^{15} photons s^{-1} at 400 eV) of this undulator beamline is ideally suited for investigations of 20 μm diameter jets produced using fused silica nozzles. The surface temperature of a 20 μm jet was measured [11] to be 0 ± 10 °C, indicating a slight thermal gradient from the middle of the jet measured to be room temperature in our laboratory. This result indicates that the liquid surface is in thermal equilibrium with the local vapour density surrounding the jet as discussed in [7, 11]. The endstation employed in these studies has been described elsewhere [7].

Total-ion-yield (TIY) and total-electron-yield (TEY) NEXAFS spectra of a 20 μm liquid jet recorded simultaneously with an instrumental resolution of 0.1 eV are shown in figure 1, along with the TIY NEXAFS spectra of water vapour. To estimate the gas-phase contribution to the liquid spectrum, the microjet was translated through the focus of the x-ray beam as shown in the inset of figure 1; this resulted in an upper bound of 20% vapour contribution. Peaks labelled A–E in the spectrum of water vapour shown in figure 1 have been previously assigned in the literature [12]. Peaks A and B result from transitions from the 1s ($1a_1$) core orbital localized on the oxygen atom to hydrogen-derived antibonding molecular orbitals $4a_1$ and $2b_2$ respectively. Under dipole selection rules, these orbitals have mainly p character. The higher-energy peaks C, D, and E originate from Rydberg states with mainly $^1B_1$, $^1B_2$, $^1B_1$ orbital symmetries respectively.

The TEY spectrum of the liquid jet is broadened into a conduction band, with the envelope of these pre-edge states blue-shifted by $\sim$1 eV relative to water vapour. These results are in agreement with previous x-ray Raman and total-fluorescence-yield studies of bulk liquid water [13, 14]. On the other hand, the TIY liquid surface measurement exhibits fully resolved peaks A, B, and C (1.1 eV FWHM) that are 10% broader and unshifted in energy relative to their gas-phase analogues. The Rydberg peaks D and E in the TIY NEXAFS are broadened into a single band which merges into the continuum. Included for comparison in figure 2 is the H$^+$ NEXAFS of amorphous ice measured by Coulman *et al* [15], clearly indicating significant differences between the surface electronic structure of liquid water and amorphous ice, despite the apparent similarities as regards the peak position of the free OH vibrational resonance.
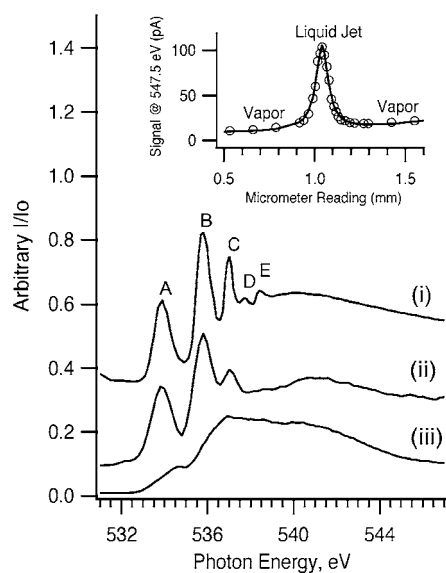
Figure 1. X-ray absorption spectra of water. (i) TIY spectra obtained from water vapour in a gas cell. NEXAFS spectra obtained from a 20 μm diameter capillary liquid jet measured by (ii) TIY and (iii) TEY techniques (offset for clarity). Inset: the liquid microjet was translated through the focused x-ray spot and the electron/ion current (at 547.5 eV) was measured as a function of jet position. The height of the x-ray beam was determined to be 80 μm FWHM. The 10× enhancement of the condensed-phase signal over emission from residual vapour demonstrates the general utility of liquid jets for obtaining high-quality liquid surface spectra without the difficult task of subtracting large background vapour signals.
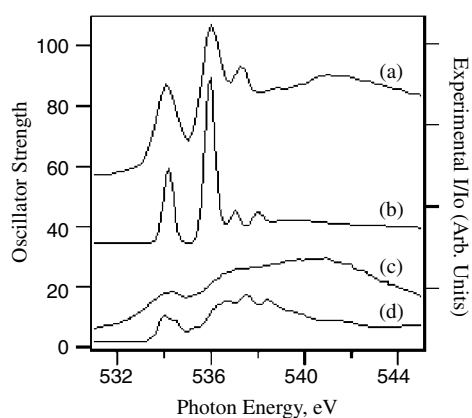

Figure 2. Experimental surface NEXAFS spectra: (a) liquid water (TIY) and (c) amorphous ice (H$^+$), measured by Coulman *et al* [15]. Spectra calculated for single-acceptor (b) and single-donor (d) hydrogen bonding surface species graphically depicted in figure 3.

To further interpret the TIY NEXAFS of the liquid microjet surface, spectra shown in figure 2 have been simulated on the basis of extended models of the water surface using the molecular orbital-based density functional theory (DFT) program deMon [16]. The three-dimensional models containing 33 water molecules, graphically depicted in figure 3, were selected to explore qualitative differences between two kinds of interfacial molecule
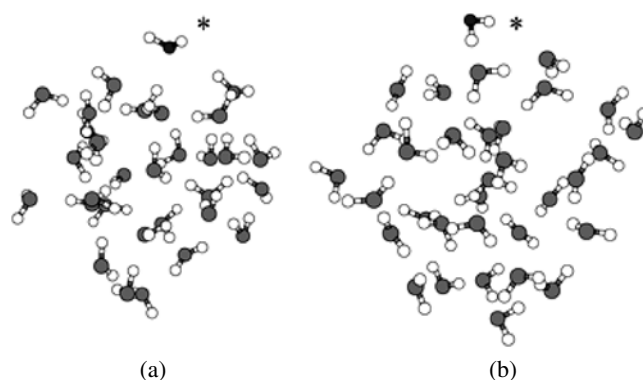
(a)   (b)

Figure 3. Three-dimensional models of two surface species (denoted with an asterisk) obtained from MD simulations: (*a*) acceptor; (*b*) donor.

coordinated to the surface through either donor or acceptor hydrogen bonds. The actual structures were taken from classical MD constant-pressure and constant-temperature (300 K) simulations of bulk water using the OSS2 potential by Ojamäe *et al* [17]. Qualitative models of the liquid surface were obtained by selecting specific configurations wherein a water molecule showed a 3 Å shortest O–O distance, as deduced from EXAFS in the surface region [7]. The surface model (figure 3) was then generated by eliminating some of the surrounding molecules. It should be noted that current simulations of the liquid/vapour interface using rigid, non-polarizable potentials do not reproduce the experimentally observed surface O–O relaxation [2, 3]. Accordingly, molecular configurations obtained from simulations of the equilibrium liquid/vapour interface using SPC/E water were used only to confirm that the conclusions drawn from the computed spectra are indeed general and do not reflect the specific cluster models selected in this work.

NEXAFS spectra were generated using the transition potential technique involving a half-occupied core hole as described in [18]. The DFT exchange and correlation functionals used were those developed by Becke [19], Perdew (and Wang) [20]. In order to simplify the definition of the core-excited centre, the oxygens of the remaining waters were described using an effective core potential (ECP) which eliminates the O(1s) level on these atoms. For the core-excited oxygen the all-electron basis set from Huzinaga [21] was used in combination with a 'double-basis-set' technique. In the latter, the molecular basis used for the energy minimization is augmented by a large (150 functions) diffuse basis set for the calculation of the transition moments and the excitation energies, yielding an improved description of the Rydberg and continuum states. The calculated oscillator strengths were then used to produce a spectrum by convoluting the data with Gaussians of full width at half-maximum (FWHM) of 0.5 eV for the region below 540 eV, a linear increase in FWHM up to 550, and FWHM 4.5 eV at higher energies. This procedure has been found to give a good representation of the NEXAFS spectra of both well-defined hexagonal ice and bulk water [13].

The experimental spectrum undoubtedly results from a distribution of water molecules with different coordination environments. However, since the spectra calculated for the donor and acceptor species show very different behaviour in peaks A, B and C, firm conclusions can still be drawn on the basis of these models. The relative intensities as well as the transition energies of the $4a_1$ and $2b_2$ antibonding molecular orbitals calculated for the single-acceptor surface molecule (figure 3) account for the major spectral features in the TIY NEXAFS of the liquid surface, providing a clear 'fingerprint' for these interfacial species. The Rydberg

peak C in the computed spectrum is split into two peaks accompanied by an overall reduction in intensity relative to the gas phase. The splitting of this peak is sensitive to the exact nature of the acceptor hydrogen bond (length, angle) and is seen in the experimental spectrum as a broadening and attenuation of peak C relative to the gas phase while the first two peaks are basically unaffected. It should be noted that the spectra calculated for double-acceptor molecules are nearly identical to the single-acceptor surface species—such that the present study cannot directly distinguish between the two. However, it is most likely that single-acceptor units will dominate the surface due to 'anti-cooperative' effects in double-donor and double-acceptor hydrogen bond configurations as reported by Ojamäe and Hermansson [22]. The donor and acceptor species, on the other hand, can be very clearly distinguished from each other.

The calculated spectrum of the single-donor species exhibits more complex near-edge fine structure accompanied by an overall reduction in the intensity of the $2b_2$ orbital relative to the $4a_1$ state. One can easily see by this comparison that the OH-derived molecular orbitals (peaks A and B) located on the donor water molecule exhibit the highest sensitivity to the presence of intermolecular hydrogen bonds. This effect has been previously observed by Myneni *et al* [13] in bulk water, where the $4a_1$ orbital is strongly influenced by the position (donor or acceptor) of the broken hydrogen bond in triply coordinated water molecules. In addition, the broad feature at ~541 eV in both the liquid and ice surface spectrum (figure 2) has been previously identified by Myneni *et al* [13] as originating primarily from more symmetric (two donor and two acceptor) hydrogen bond configurations.

Previous studies of water monomers, clusters, and amorphous ice have all shown that the TIY NEXAFS spectra arise exclusively from *free OH bonds* located either in free water molecules or on an ice surface. Specifically, Coulman *et al* [15], observed that H^+ dominates the TIY from amorphous ice with a 10^3 enhancement over molecular and cluster ions. This result, in addition to polarization studies, led them to conclude that the H^+ emission, produced by an ultrafast dissociation mechanism, originated from surface molecules possessing one free OH bond. Recent photoelectron–photoion coincidence studies support this picture [23]. These results imply that interfacial H_2O molecules with two free O–H bonds (as in the pure acceptor configuration) will dominate the pre-edge TIY NEXAFS spectrum of the liquid surface. Conversely, the donor configuration, in which there is a single free OH bond, is more representative of the surface of amorphous ice as well as the liquid side of the water interface, as probed by SFG [24]. The simulations presented here can account for the main pre-edge spectral features observed in amorphous ice by Coulman *et al* [15] (figure 2) and are consistent with the single-donor species previously detected by infrared spectroscopy [25].

These x-ray absorption results clearly identify a new population of interfacial molecules in addition to the single-donor configurations previously observed by SFG studies. The observation of these acceptor-only species in dynamic equilibrium with the vapour is facilitated by the sub-femtosecond timescale of core-level excitation, allowing the direct observation of instantaneous local hydrogen bond configurations. We speculate that there may be a dynamic interplay between the single-donor and acceptor-only molecules that affords insight into the molecular details of evaporation. Simply, single-donor molecules can interconvert to acceptor-only configurations by breaking a single hydrogen bond via a librational motion after which the molecule would be liberated from the liquid surface. If this picture is correct, condensation would then be achieved by surface capture of gas-phase molecules through the initial formation of an acceptor hydrogen bond. This proposed mechanism is contrasted with condensation dynamics observed in amorphous ice in which vapour molecules are captured with the highest probability by forming two hydrogen bonds (one acceptor, one donor) as

reported by Zhang and Buch [26]. These respective mechanisms could reflect the inherent differences in the surface electronic structure of ice and liquid water observed in this work. Such details would have obvious implications for the molecular understanding of gas-phase transport of solute molecules into aqueous solutions, important for many problems in heterogeneous chemistry.

References

[1] Brauslau A, Deutsch M, Pershan P S and Weiss A H 1985 *Phys. Rev. Lett.* **54** 114
[2] Townsend R M and Rice S A 1991 *J. Chem. Phys.* **94** 2207
[3] Dang L X and Chang T M 1997 *J. Chem. Phys.* **106** 8149
[4] Taylor R S, Dang L X and Garrett B C 1996 *J. Phys. Chem.* **100** 11 720
[5] Alejandre J, Tildesley D J and Chapela G A 1995 *J. Chem. Phys.* **102** 4574
[6] Du Q, Superfine R, Freysz E and Shen Y R 1993 *Phys. Rev. Lett.* **70** 2313
[7] Wilson, Kevin R, Rude B S, Catalano T, Schaller R D, Tobin J G, Co D T and Saykally R J 2001 *J. Phys. Chem.* B **105** 3346
[8] Bianconi A 1980 *Appl. Surf. Sci.* **6** 392
[9] Seiger M T, Simpson W C and Orlando T M 1997 *Phys. Rev.* B **56** 4925
[10] Tolk M, Traum M, Tully J C and Madley T E 1982 *Desorption Induced by Electronic Transitions DIET-I* (Berlin: Springer) and references therein
[11] Faubel M, Steiner B and Teonnies J P 1988 *Z. Phys.* D **10** 269
[12] Kim D Y, Lee K, Ma C I, Mahallingam M and Hanson D M 1992 *J. Chem. Phys.* **97** 5915
[13] Myneni S *et al* 2002 *J. Phys.: Condens. Matter* **14** L213
[14] Brown D T *et al* 2000 *Phys. Rev.* B **52** R9223
[15] Coulman D, Puschmann A, Hoffer U, Steinruck H P, Wurth W, Feulner P and Menzel D 1990 *J. Chem. Phys.* **93** 58
[16] Pettersson L G M *et al* 2001 *deMon Software 2001*
[17] Ojamäe L, Shavitt I and Singer S J 1998 *J. Chem. Phys.* **109** 5547
[18] Triguero L, Pettersson L G M and Ågren H 1998 *Phys. Rev.* B **58** 8097
[19] Becke A D 1998 *Phys. Rev.* A **38** 3098
[20] Perdew J P 1986 *Phys. Rev.* B **33** 8822
[21] Huzinaga S J 1965 *J. Chem. Phys.* **42** 1293
[22] Ojamäe L and Hermansson K 1994 *J. Phys. Chem.* **98** 4271
[23] Mase K, Nagasono M, Tanaka S, Urisu T, Ikenaga E, Sekitani T and Tanaka K 1997 *Surf. Sci.* **390** 97
[24] Morita A and Hynes J T 2000 *Chem. Phys.* **258** 371
[25] Devlin J P 2000 *J. Chem. Phys.* **112** 5527
[26] Zhang Q and Buch V 1990 *J. Chem. Phys.* **92** 1512